

CONTENTS	
INTRODUCTION.....	
1. Metal complexes of biological interest.....	
1.1 Biological activity of metals.....	
1.2 Biological activity of metal complexes with ligands of biological interest.....	
2. Experimental methods of investigation of molecular complexes.....	
2.1 Elemental chemical analysis.....	
2.2 Atomic Absorption.....	
2.3 Thermogravimetric analysis(TG).....	
2.4 Analysis Differential scanning calorimetry (DSC).....	
2.5 Electronic Spectroscopy.....	
2.6 Fourier Transform Infrared Spectroscopy (FT-IR).....	
2.7 Electron Spin Resonance (RES).....	
2.8 Introduction to Raman vibrational spectroscopic techniques.....	
3. Metal complexes with phenylalanin as a ligand.....	
3.1 Introduction.....	
3.2 Synthesis of metal complexes with phenylalanine.....	
3.3 Methods of investigation of metal complexes.....	
3.4 Partial conclusions.....	
4. Spectroscopic and theoretical studies on the amoxicillin molecule.....	
4.1 Introduction.....	
4.2 Computational methods for investigating molecular structure.....	
4.3.....	
4.4 Partial conclusions.....	
Conclusions.....	
Bibliography.....	

## INTRODUCTION

Metal ions fulfill some important functions in living organisms or have on them different actions. In general, metal ions can be found in living organisms or they act inside them in the form of complexes or by forming complexes, chelates generally, the complex ion generator is involved in the formation of chelate cycles. The participation of metal ions in biological processes consists in their contribution and breaking of chemical bonds, the charge transfer and oxygen, to nitrogen fixation in photosynthesis, to maintain osmotic balance in multiphase systems and enzymatic reactions. The main spectroscopic methods used to determine the vibrational modes in molecules is based on infrared absorption processes and Raman scattering.

The most common techniques to investigate the vibrational energy structure are IR absorption spectroscopy and Raman scattering. The IR absorption the substance is irradiated with a broad spectrum of frequencies in the middle IR spectral range; from interaction with molecules absorb photons whose energy is the difference between two vibrational energy levels. When Raman scattering is used monochromatic radiation, a laser, photons suffer elastic and inelastic collisions with molecules. In Raman spectroscopy are analyzed wavelengths of inelastic scattered photons, they provide information on vibrational modes of molecules. These methods are used mainly to obtain information on chemical structure and physical form, to identify substances with characteristic spectra as well as quantitative and semiquantitative determination of a sample of substance. Also in the field of infrared spectroscopy (IR) is a suitable method for identifying the presence of functional groups of molecular structure of organic compounds. Spectroscopy can be divided into several branches, depending on the wavelength spectrum of electromagnetic radiation considered. So, we have microwave spectroscopy, infrared, visible and ultraviolet. Depending on the type of transition involved in the emission or absorption spectroscopy we talk about rotation, vibration, electronic and ionization spectroscopy. There is a type of spectrum that does not involve any process of absorption or emission. Raman spectroscopy is about studying the scattered radiation (scatter) of the sample. The radiation source may be visible, near ultraviolet or near infrared.

The SERS effect was accidentally discovered in 1974 while researchers tried to obtain the Raman signal on an electrode. The original idea was to generate a large surfaces on a rough

metal. Gradually researchers realized that the surface area is not the key to this phenomenon. After a search period, the progress took place in 1977 when two groups of researchers have found that raw silver electrode produces a Raman spectrum which is a million times more intense than normal Raman spectrum. This enormously powerful signal started to surface enhanced Raman scattering (SERS). Currently, SERS overcomes the disadvantage of small scattering cross section of Raman spectroscopy, and can even be used to obtain Raman signal from a single molecule.

## **1. Metal complexes of biological interest**

Current development of science and technology relies mostly on the possibility of obtaining various materials with properties destined to meet various practical purposes. This possibility is mainly based on the correlation between synthesis and physicochemical properties of materials.

Structural analysis aims to form a correct image on the matter, in general, and substance, in particular, through an unified presentation of the structural parameters that characterize the chemicals by indicating the physical methods used in investigating the structure of substances and the logical presentation of the physical parameters review and investigation methods used.

The link between physical and chemical properties of substances and their structure and causes stems from how substances interact with each other, and radiation fields on the structure of atoms, molecules and crystals which are formed [1].

The study should determine the physical properties of substances (characteristics measured and expressed numerically), chemical properties (or chemical reactions), the qualitative and quantitative composition (nature and proportion of elements) and structure, ie the arrangement of structural components from each ie other molecules, atoms and ions.

### 3. PHENYLALANINE METAL COMPLEXES LIGAND

#### 3.1 Introduction

In recent years the importance of metal ions for the proper operation of plant and animal organisms, was highlighted by the publication of numerous papers in biophysics and biochemistry. New research in these areas focuses on the synthesis and characterization of biological compounds containing metal ions, due to their applicability in pharmacy, medicine, agronomy and nutrition [1]. Biological processes involving compounds formed by various elements of the biological substrate regularly. Animal and vegetable bodies are composed of chemicals with a complex composition, being composed of both metal and non-metals. Chemical elements that are part of living matter are selected by nature, by certain principles that are not yet well understood, but it can be said with certainty, that their spread in the environment is not the decisive element.

The complexity and diversity of peptides and proteins is due to the large number of alternative binding of a small number of  $\alpha$ -amino for their formation and specific features of the conformation and configuration of their molecules. They are generated by alternating rigid planar elements (link polyamide conjugated) structure with elements of mobility ( $sp^3$  hybridized carbon atoms) capable of generating chirality axis. In addition, the possibility of establishing connections (van der Waals, hydrogen, dipole-dipole, induction, inter and intra molecular dispersion) leads to stabilization of conformation as well individualized entities.

Alpha amino acids with transition metals form complexes or chelates internal color, hard soluble and stable. Divalent metals such as Mn (II), Cu (II) and Ni (II) can form metal coordination compounds in which amino acid binds two molecules of nitrogen and oxygen by making frequent coordination number of four one-square plan configuration pseudotetrahedral. Trivalent metals such as Fe (III), Co (III) can form complex salts with three amino acid molecules in the metal coordination number six is made.

### 3.2 The synthesis of metal complexes with amino acids

The synthesis of metal coordination compounds with Cu (II), Co (II) and Zn (II) with henylalanine takes place in three stages:

- a) preparation of metal salt solution;
- b) preparing the ligand solution;
- c) the actual synthesis and purification of the obtained compounds;

The synthetic route we chose is based on one proposed by Lancashire [104], and seeks neutral complex type  $ML_2 \cdot nH_2O$  at a pH between 8 and 10 when in the presence of strong bases can be achieved conditions of amino acid ionization

#### 3.2.1 The synthesis of copper complexes

We weight 2 mmol of amino acid (0.320 g L and 0.262g L) and are dissolved in a minimum volume of distilled water (max.5ml). We calculate the volume of 6M NaOH needed to replace a proton from each mole of amino acid (0.33ml) and added in drops over the amino acid solution. We weight the equivalent amount of a mmol of cupric salt. When using cupric nitrate,  $Cu(NO_3)_2 \cdot 3H_2O$ , 0.241g weighed and dissolved in 2 ml distilled water. We add the salt solution over cupric amino acid solution and shake for several minutes with the magnetic stirrer. The precipitate is filtered, washed with ethanol and allowed to dry at room temperature, then kept in closed containers to carry out the necessary analyzes.

Table nr. 1.3 Complexes of Cu (II) with phenylalanine

<i>Compound</i>	<i>Symbo</i>	<i>Colour</i>	<i>Yield</i>	<i>Melting Point</i>
$Cu(\text{fenilalanina})_2 \cdot H_2O$	Cu-L	Greeniesh blue	98.6%	220 °C

#### 3.2.2 The synthesis of cobalt complexes

We weight 2 mmol of amino acid (0.330 g L and 0.286 g L) and are dissolved in a minimum volume of distilled water (max.5ml). We calculate the volume of 6M NaOH needed to replace a proton from each mole of amino acid (0.33ml) and added in drops over the amino acid

solution. We weight 0,238 g of cobalt salt and are dissolved in 2 ml distilled water. We add the above amino acid solution and shake for several minutes on the magnetic stirrer. The precipitate obtained when Co-L complex is filtered, washed with ethanol and allowed to dry at room temperature, then kept in closed containers to carry out the necessary analyzes.

Table nr. 2.3 Complexes of Co (II) with phenylalanine

<i>Compound</i>	<i>Symbol</i>	<i>Colour</i>	<i>Yield</i>	<i>Melting Point</i>
<i>Co(fenilalanina)<sub>2</sub>·2H<sub>2</sub>O</i>	Co-L <sub>1</sub>	Purple-light	54.4%	255 °C

### 3.2.3 The synthesis of zinc complexes

We weight 2 mmol of amino acid (0.320 g L and 0.286 g L) and dissolve in hot distilled water (5ml). We calculate the volume of 6M NaOH needed to replace a proton from each mole of amino acid (0.33ml) and added in drops over the amino acid solution. We weight the equivalent amount of zinc salt ZnSO<sub>4</sub>·7H<sub>2</sub>O mmol (0.287g) and dissolve in distilled water, then add more amino acid solution and shake for several minutes on the magnetic stirrer. The precipitate is filtered, washed with ethanol and allowed to dry at room temperature, then kept in closed containers to carry out the necessary analyzes.

Table nr. 3.3 Complexes of Zn with phenylalanine

Compound	Symbol	Colour	Yield	Melting Point
Zn(fenilalanina) <sub>2</sub> ·H <sub>2</sub> O	Zn-L <sub>1</sub>	White Amorphous	94.4%	175 °C

### 3.3 Methods of investigation of metal complexes

This part contains chapters synthesis and sample preparation for analysis and various physico-chemical, thermal and spectroscopic investigation of metal complexes to determine: The coordination of a metal ion with ligands:

1. a local structure change depending on the ligand
2. a change in local symmetry around the paramagnetic ion
3. a presence of dimeric specie

Steps taken to date can be summarized as follows:

Synthesis	<ul style="list-style-type: none"> <li>♣ Establishment of synthesis conditions for obtaining metal compounds with different amino acid ligands</li> </ul>
Characterization of compounds of biological interest	<ul style="list-style-type: none"> <li>♣ Basic chemical analysis</li> <li>♣ Atomic Absorption Spectroscopy</li> <li>♣ Thermal analysis               <ul style="list-style-type: none"> <li>- Analysis of thermogravimetric</li> <li>- Differential Thermal Analysis</li> </ul> </li> <li>♣ Study in the IR spectra</li> <li>♣ Study in Ultraviolet spectra (UV) and Visible</li> <li>♣ Study of electron spin resonance spectra (ESR)</li> </ul>

Experimental design:

Elemental analysis was performed using a Vario El device that allows quantitative determination of carbon, nitrogen, hydrogen, sulfur and oxygen in different modes of operation CHN, CNS, CN, CHSN, CHNSO. Atomic mass absorption measurements were performed with a AAS-1 at wavelength = 320 nm. Samples were prepared as follows: To weigh an amount of 0.02 g of complex, which was dissolved in few milliliters of distilled water.

Were added 5 ml 35% HCl to break down complex. The solution was completed to 100 ml with distilled water, the solution was diluted 1:2. Ultraviolet and visible spectra were recorded with a Jasco-V-530 spectrophotometer at wavelengths between 190 and 800 nm.

Thermal behavior of copper complexes was determined by recording curves of thermolysis with a Q-1500D derivatographic, the 200C-5000C temperature range, with a constant heating rate 100C/minut. Samples were considered masses between 100-300mg. Differential scanning calorimetric analysis (DSC) were performed with a Metler-Toledo, using aluminum crucibles containing samples whose masses were investigated between 1 and 2.5 mg. The measurements took place between 20 -500 0C, the heating rate being 100C/minut.

Electronic spectra were determined with a Jasco V-530 spectrophotometer with wavelengths between 190-800nm. If ligands were prepared 10<sup>-4</sup>M concentration solutions by dissolving them in double distilled water. Solutions were prepared with 10<sup>-3</sup>M concentrations of complexes by dissolution in water, methanol or ethanol, depending on the solubility of each in these solvents. Some cases have required dilution to be seen in the UV transitions more characteristic of ligands.

Recording spectra in the infrared was done using a Perkin-Elmer FTIR 1730 spectrophotometer in KBr tablets in the range 4000-400 cm<sup>-1</sup>. Electron spin resonance spectra were recorded with a standard spectrometer Depth PS8400 Portable EPR Spectrometer at 9.56 GHz on solid samples in aqueous solutions at room temperature.

### 3.3.1 Investigation of metal complexes with phenylalanine as ligand

Phenylalanine (L) (C<sub>6</sub>H<sub>5</sub>CH<sub>2</sub>CHNH<sub>2</sub>COOH) is an essential aromatic amino acid, which contains a benzene ring, so it is hydrophobic. The body converts phenylalanine into tyrosine, another amino acid essential for the proper functioning of the brain, thyroid hormones, etc.. Deficiency of phenylalanine causes confusion, lack of energy, reduced storage capacity and decreased appetite [45]. There is a metabolic disease called phenylketonuria is a genetic disease fenilalaninhidroxilază or missing enzyme has a very low level in blood (PAH). This enzyme is needed to convert phenylalanine into another amino acid called tyrosine. If PKU is not treated immediately after birth, phenylalanine builds up in blood and brain tissue leading to mental retardation and central nervous system.

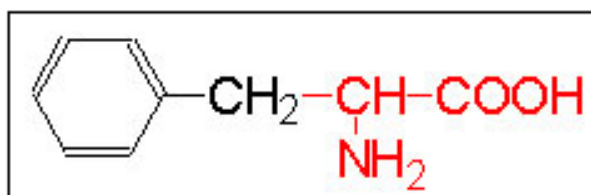


Fig.6.3 Structural formula of phenylalanine

### 3.3.1.1 Chemical analysis and atomic absorption elemental mass

The results of elemental analysis and atomic absorption mass confirms composition 1: 2 metal: phenylalanine. Data are presented in Table 4.3.

Table 4.3 Elemental analysis results for the complexes synthesized

Complex	Molec. weight	% Experimental / calculated			
		C	H	N	Metal
$Cu(L)_2 \cdot H_2O$	407.92	53.40 (53.00)	4.72 (4.94)	7.00 (6.86)	15.82 (15.57)
$Co(L)_2 \cdot 2H_2O$	389.4	51.42 (55.46)	8.59 (8.2)	8.28 (7.59)	20.41 (19.17)
$Zn(L)_2 \cdot H_2O$	395	51.85 (54.69)	9.07 (8.10)	6.57 (7.08)	14.52 (15.25)

### 3.3.1.2 Analysis of thermogravimetric

Derivatograma copper complex with phenylalanine (Fig. 7.5) has a horizontal plateau up to 1700C, corresponding endothermic effect when a large mass loss of 80.5% (83.7% theoretical), indicating the breakdown of amino acid molecules.

After 250 0C thermolysis curve shows a steady decline, indicating the formation of CuO residue for which the mass loss is 19.5% derivatograma and theoretical is 19.25%. Decomposition of the complex is a small temperature range, starting at 350<sup>0</sup>C [46-48].

Table 5.3 Results of thermogravimetric analysis

Complex	Peak DTG ( $^{\circ}C$ )		Loss of weight TG (%)		Assignment
	Endo	Exo	Endo	Exo	
[Cu(L) <sub>2</sub> ] H <sub>2</sub> O	105	-	4.39	4.45	A molecule of water of crystallization.  Melting point Rest Ogan 2C <sub>7</sub> H <sub>7</sub> 2C <sub>2</sub> H <sub>3</sub> NO <sub>2</sub> residue CuO
	255	-	-	-	
	-	320	44.46	44.52	
	-	470	35.64	35.15	
			15.50	15.86	

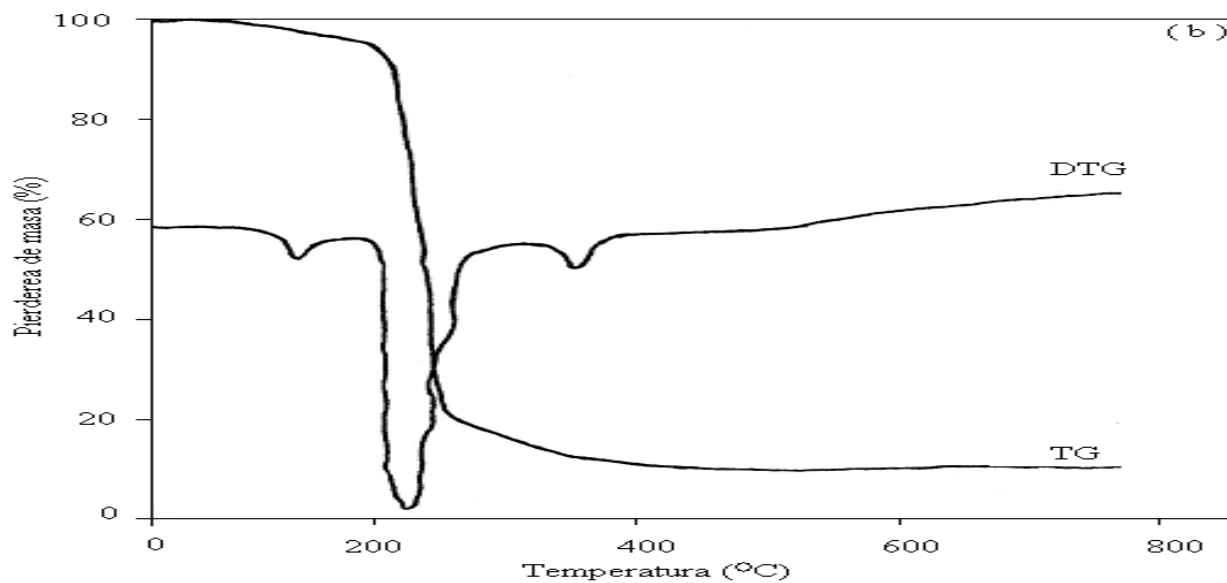


Fig. 7.3 thermograms complex Cu-L [170]

### 3.3.1.3 Differential thermal analysis

In the figure above (Fig.8.5.a) DSC curve is shown in the standard of phenylalanine (L), which presents a first step a glassy transition, which is an endothermic process with a maximum at 170 °C [109]. Phenylalanine melting occurs with decomposition, between 220 °C and 260 °C, with an endothermic maximum at 240 °C and complete combustion takes place after 450 °C

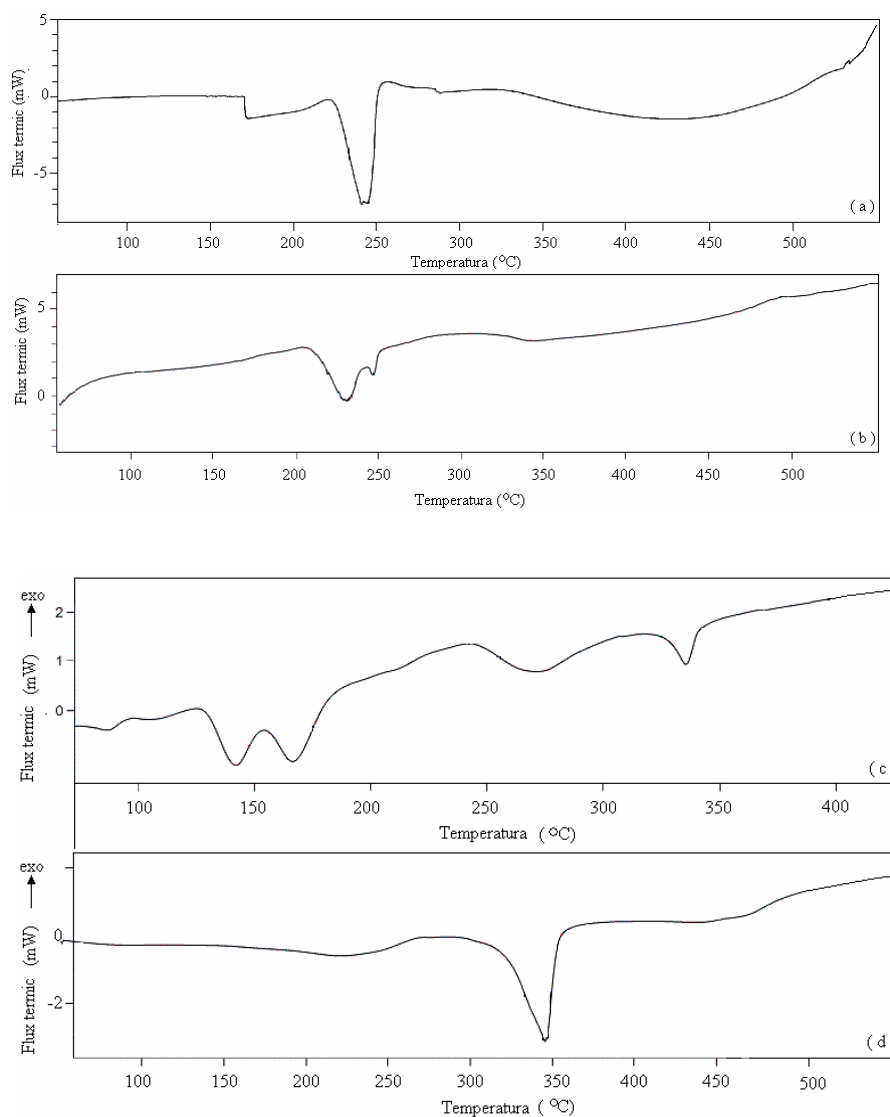


Fig. 8.3 DSC curves of L (a), Cu-L (b), Co-L (c) and Zn-L (d)

Complex Cu-L suffers between 100 and 180 °C glassy transition process followed by endothermic decomposition in two successive steps with maxima at 230 °C and 250 °C. This is due to formation of intermediate degradation process. At 300 °C is shown exothermic peak of crystallization process, followed by pyrolysis at 450 °C copper complex [49]. Complex Zn-L (Fig.8.5.d) has better thermal stability than the corresponding ligand and copper complex. DSC curve of this complex has a melting process of decomposition between 295 °C and 320 °C followed by complete combustion as 450 °C.

### 3.3.1.4 FT-IR Spectroscopy

FT-IR spectra of phenylalanine (L) (Fig.6.3.a) presents stretching vibration band characteristic of the NH bond, split into two signals at 3078  $\text{cm}^{-1}$ , 3030  $\text{cm}^{-1}$  respectively. This band is shifted to 3320  $\text{cm}^{-1}$  or 3256  $\text{cm}^{-1}$  in the spectrum of complex Cu-L, which proves the involvement of amino group in complex formation. In the case of cobalt and zinc complexes this band is shifted to 3220  $\text{cm}^{-1}$  and 3334  $\text{cm}^{-1}$ , 3256  $\text{cm}^{-1}$  suggesting that the amino group also involved the formation of these complexes [46,50]. Group deformation vibration of  $\delta$  (NH) appears at 1557  $\text{cm}^{-1}$  in the ligand spectrum and are shifted to 1567  $\text{cm}^{-1}$  for Cu-L, 1586  $\text{cm}^{-1}$  for Co-L respectively 1561  $\text{cm}^{-1}$  for Zn-L as also explains the involvement of this group to bond formation with the metal [51]. Stretching vibration  $\nu$  (C = O), of which we are especially interested in, is where the 1623  $\text{cm}^{-1}$  ligand and is shifted by 4  $\text{cm}^{-1}$  (Cu-L) and 9  $\text{cm}^{-1}$  (for Zn-L) which demonstrates carboxyl group to form covalent bond with the metal ion. If the cobalt complex characteristic band  $\nu$  (C = O) appears at 1633  $\text{cm}^{-1}$  and not well resolved, the presence of this band can be attributed to hydrogen bond formation between carboxyl groups and water or involvement in coordination.

According to literature [52] at 603  $\text{cm}^{-1}$  and 468  $\text{cm}^{-1}$  bands should appear corresponding  $\rho$  (COO-) Pending these bands in the spectrum of the complexes, indicating metal ion binding to carboxyl groups, unfortunately the spectra below these bands cannot be viewed spectrofotometrului

Because phenylalanine has a cycle structure of benzene, the IR spectrum of stretching vibrations of the cycle to be found in two fields of frequencies up to  $745\text{ cm}^{-1}$  and  $1495\text{ cm}^{-1}$ . If metal complexes with the ligand phenylalanine aromatic cycle characteristic bands are shifted lightly or not at all. Characteristic band  $\nu(\text{OH})$  appears in the spectrum at  $3454\text{ cm}^{-1}$  complexes, respectively  $3453\text{ cm}^{-1}$  and  $3359\text{ cm}^{-1}$  indicating the presence of water molecules of crystallization [53].

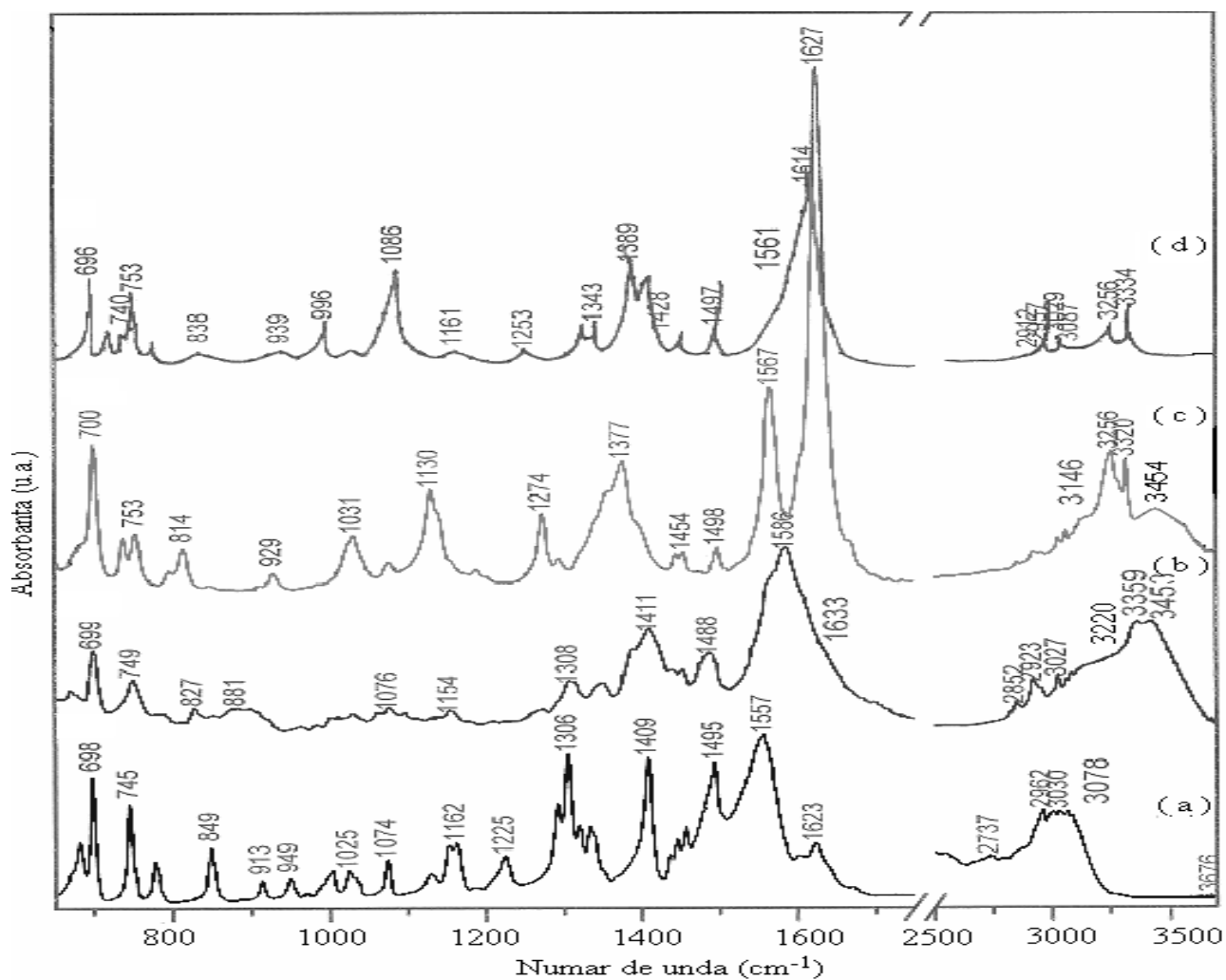


Fig.6.3 Spectrul FT-IR al L (a), Cu-L(b), Co-L (c) și Zn-L (d)

Tabel 6.3 *Datele spectrale FT-IR (cm<sup>-1</sup>)*

$\nu(N-H)$	$\nu(C=O)$	$\delta(N-H)$	$\nu(O-H)$	Compus
3078 3030	1623	1557	-	L
3320 3256	1629	1567	3454	Cu- L
3220	1633	1586	3453 3359	Co- L
3334 3256	1614	1561	-	Zn- L

### 3.3.1.5 UV-VIS spectroscopy

Phenylalanine is part of the aromatic amino acid, threonine and tyrosine together, these three amino acids are responsible for the fluorescent properties of proteins. Aromatic amino acids absorb UV light around 250-300 nm region as follows: threonine at 280 nm, tyrosine and phenylalanine from 274 nm to 257 nm. Absorbivitatea mole of tryptophan is five times higher than the tyrosine and 50 times higher than that of phenylalanine [54]. It is important to mention that protein absorption in the range 275-280 nm, is due almost entirely to these three amino acids.

If phenylalanine our study shows that it has the 231 nm band due to  $n \rightarrow \pi^*$  transition characteristic of group C = O. This spectrum is shifted to 225 nm complexes (Cu-L), 235 nm (Co-L) respectively at 220 nm (Zn-L) confirmed the presence of ligand in the complex nature of the covalent link [55-57]. The UV spectrum (Fig.7.5.a) of phenylalanine, characteristic band  $\pi \rightarrow \pi^*$

transition occurs at 260 nm and is shifted by 15 nm range complexes (Cu-L), 20 nm (Co-L) and 7 nm (Zn-L) and is assigned to conjugated systems. But in the visible spectrum of copper complex present in 615 nm band corresponding to the transition  $2T_{2g} \rightarrow 2E_g$  specific copper complexes with distorted tetragonal symmetry due to Jahn-Teller. Complexul effect of cobalt present in the visible band at 540 nm, which assigned transition  $4T_{1g}(P) \rightarrow 4T_{1g}(F)$  [58].

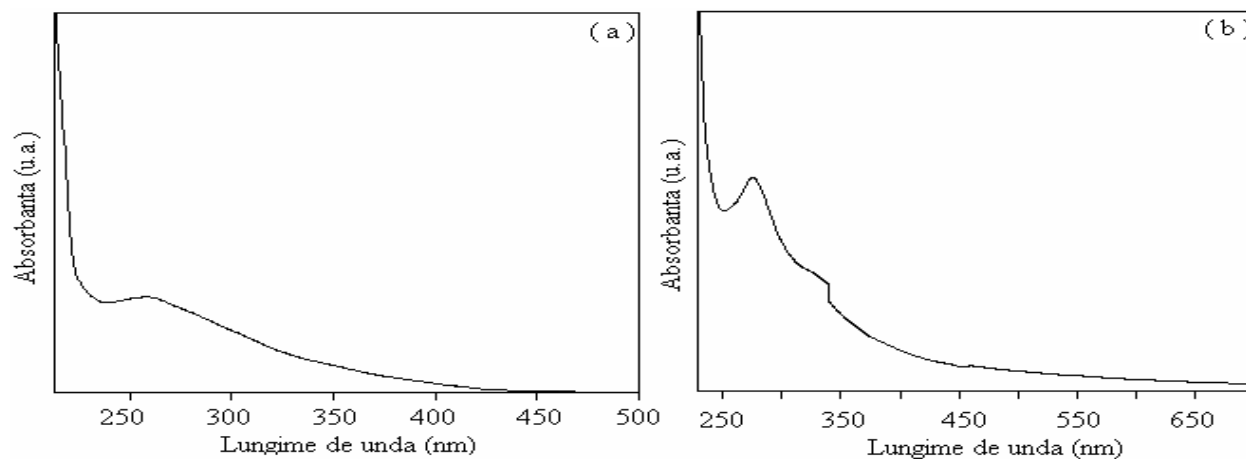


Fig. 7.3 Spectrul UV al L (a) și Cu-L(b)

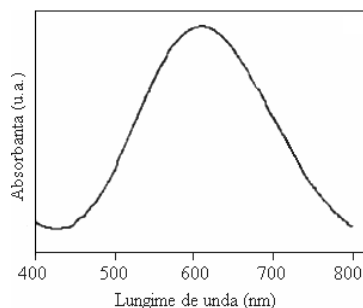


Fig. 8.3 Spectrul VIS al complexului Cu-L în DMF

### 3.3.1.6 Electron Spin Resonance Complex

Spectrum of copper (Fig.9.3.a) performed at room temperature on polycrystalline powders, is typical of monomeric species pseudotetraedrale. Tensors values giromagnetici:  $g_{\parallel} = 2.197$ ,  $g_{\perp} = 2.209$  corresponding to a chromophore  $\perp$   $CuN_2O_2$ .

ESR spectra of Cu-phenylalanine complex solution (10 mg DMF complex / 0.5 ml DMF) (Fig.9.5.b) contains lines characteristic isotropic hyperfine structure ( $g_0 = 2.124$ ,  $A_0 = 82$  G) [46,55,56].

Solution isotropic spectrum were seen in the resolution of the four signals corresponding to hyperfine interaction between electron paramagnetic metal ion nucleus ( $I_{Cu} = 3/2$ ). The values of  $A_0$  and spectra corresponding to a specific form pseudotetrahedral symmetry around the metal ion [57]. If we obtained cobalt complex EPR spectrum at room temperature, which reveals the presence of a compound monomer ( $g = 2.195$ ), with octahedral symmetry around the cobalt ion.

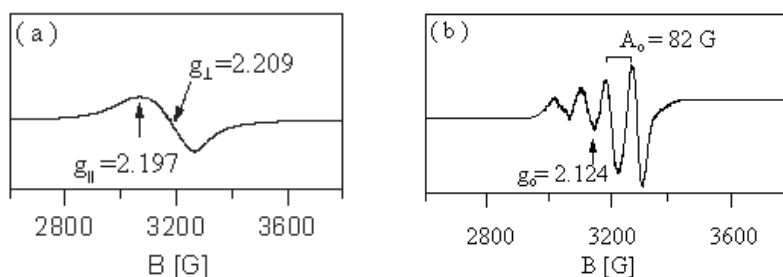


Fig.9.3 ESR spectrum of complex 1 powder (a) and DMF (b)

### 3.3.1.7 The proposed structures

Three metal complexes have been synthesized in aqueous solution  $[Cu(L)_2] \cdot 2H_2O$ ,  $[Cu(L)_2] \cdot 2H_2O$  and  $[Cu(L)_2] \cdot H_2O$  and investigated by physico-chemical, spectroscopic and thermal. According to available data we propose the three complex formulas, which are shown in Figure 10.5. As shown, copper and zinc complexes have a compass around pseudotetrahedral metal ion and complex cobalt has octahedral symmetry around the cobalt ion.

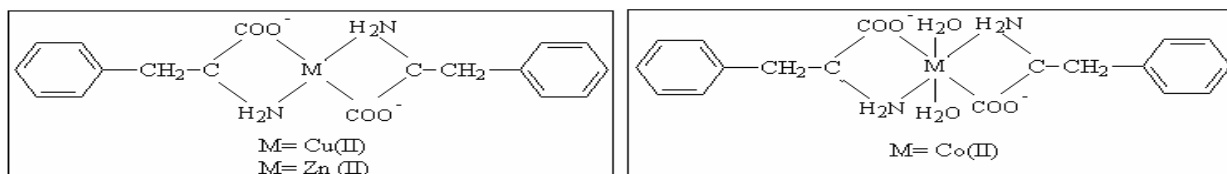


Fig. 10.3 Structural formulas proposed for complexes of phenylalanine

### 3.4 Partial Conclusion

In this part of the work we studied the amino coordinative ability towards some 3d transition metal ions. Metal complexes were synthesized in November:  $[\text{Cu}(\text{L})_2] \cdot \text{H}_2\text{O}$ ,  $[\text{Co}(\text{L})_2] \cdot 2\text{H}_2\text{O}$  and  $[\text{Zn}(\text{L})_2] \cdot \text{H}_2\text{O}$  with phenylalanine and characterized by physicochemical methods: elemental analysis, spectroscopy mass absorption, thermal: thermogravimetric analysis and differential calorimetric and spectroscopic analysis: IR spectroscopy, UV-VIS and ESR.

Preparation of metal-amino acid complexes of 1:2 is based on their synthesis in an alkaline environment and deprotonation of carboxyl groups of molecules covalent ligands for establishing links and coordination with metal ions. A simple amino acid anion is a potential bidentate ligand, which may coordinate to a transition metal ion, a carboxyl and amino groups by able to donate electrons to form a heterocyclic ring structure.

Elemental analysis and atomic absorption measurements confirm the stoichiometry resulting table type metal complexes  $[\text{M}(\text{L})_2] \cdot x\text{H}_2\text{O}$  ( $\text{M} = \text{Cu}(\text{II}), \text{Co}(\text{II})$  and  $\text{Zn}(\text{II})$  and  $X = 1$  for  $\text{Cu}$  and  $\text{Zn}$  and  $X = 2$  for  $\text{Co}$ ). Thermal behavior of complexes studied is similar, ranging in weight by removing water of crystallization, decomposition of the complex in one or more steps and metal oxide formation. Processes accompanying loss of crystallization water molecules or complexes are endothermic decomposition and the rearrangements occurring in the molecule, formation of new connections or burnt, are exothermic effects. By comparing the IR spectra of the ligand with the synthesized compounds have established coordination mode to metal centers, namely the amino nitrogen atom and oxygen atom of carboxyl group.

Also, analysis of vibration bands at about  $3600 \text{ cm}^{-1}$  allowed the determination of the number of water molecules which coordinates the metal center. Were identified and assigned to the main vibration bands of significant molecular groups. IR spectra indicate bidentate character of the ligand and allowing a local geometry pseudotetraedrale for ions  $\text{Cu}(\text{II})$  and  $\text{Zn}(\text{II})$  and one for octahedral complexes of  $\text{Co}(\text{II})$  synthesized. According to those obtained from thermal and ultraviolet and visible spectroscopy, we can say that the local octahedral symmetry for ions

Co (II) coordination is done by the axial position of two water molecules. EPR spectra recorded on powders of metal complexes-ligand covalent bonds confirm formats pseudotetraedrală local geometry around the metal ion Cu (II) and Zn (II) and octahedral ions Co (II).

## 4. Spectroscopic and theoretical studies on the amoxicillin molecule

In this work a joint experimental and theoretical study on amoxicillin is reported. The molecular vibrations of amoxicillin were investigated by FTIR, FT-Raman and SERS spectroscopies. In parallel, quantum chemical calculations based on density functional theory (DFT) are used to determine the geometrical, energetic and vibrational characteristics of the molecule with particular emphasis put on the interaction and adsorption geometry of the molecule to the silver colloidal surface. The SERS spectrum of amoxicillin was recorded using a 532 nm laser line and hydroxylamine reduced silver colloid as SERS substrate. FTIR, FT-Raman and SERS spectra of amoxicillin were assigned based on DFT calculations with the hybrid B3LYP exchange-correlation functional, coupled with the standard 6-31G(d) basis set. The calculated molecular electrostatic potential was used in conjunction with SERS data to predict the adsorption geometry of the molecule on silver colloid.

### 4.1 Introduction

Amoxicillin belongs to a class of antibiotics called penicillin. Amoxicillin is a moderate-spectrum, bacteriolytic,  $\beta$ -lactam antibiotic used to treat bacterial infections caused by susceptible microorganisms. Amoxicillin is effective against many different bacteria including *H. influenzae*, *N. gonorrhoea*, *E. coli*, *Pneumococci*, *Streptococci*, and certain strains of *Staphylococci*. It is usually the drug of choice within the class because it is better absorbed, following oral administration, than other  $\beta$ -lactam antibiotics. It acts by inhibiting the synthesis of bacterial cell wall, which are necessary to protect bacteria from their environment.

Due to the bio-molecular relevancy of amoxicillin, several spectroscopic studies can be found in the literature. A physicochemical characterization of amoxicillin and its beta-cyclodextrin complexes is shown in a recent study [1], including FTIR and NMR spectroscopy. Other spectroscopic methods employed for amoxicillin molecular characterization include, fluorescence [2], Raman and SERS [3].

Analytical detection approaches include UV spectrophotometry for amoxicillin determination in urine [4], NIR absorption combined with chemometrics as a method for the

nondestructive determination of compound amoxicillin powder drug [5], chemo-luminescence [6] for determination of the compounds in pharmaceutical formulations and spiked plasma samples, or LC-MS/MS determination of amoxicillin in human plasma [7].

In the present study IR and Raman spectra of amoxicillin were assigned based on DFT calculations based on the hybrid B3LYP exchange-correlation functional, coupled with the standard 6-31G(d) basis set. The adsorption geometry of the amoxicillin molecule on colloidal silver surface was deduced from the SERS selection rules and the analysis of the calculated molecular electrostatic potential (MEP).

#### **4.2 Computational methods for investigating molecular structure**

The FTIR spectrum of amoxicillin powder was recorded at room temperature on a conventional Equinox 55 (Bruker Optik GmbH, Ettlingen, Germany) FTIR spectrometer equipped with an DTGS detector and an ATR setup with ZnSe crystall.

The FT-Raman spectrum was recorded in a backscattering geometry with a Bruker FRA 106/S Raman accessory equipped with a nitrogen cooled Ge detector. The 1064 nm Nd:YAG laser was used as excitation source, and the laser power measured at the sample position was 300 mW. All spectra were recorded with a resolution of  $4\text{ cm}^{-1}$  by co-adding 32 scans.

The SERS spectrum was recorded using a DeltaNu Advantage spectrometer (DeltaNu, Laramie, WY) equipped with a doubled frequency Nd:YAG laser emitting at 532 nm. The laser power was 40 mW and the spectral resolution  $10\text{ cm}^{-1}$ .

All chemicals used were of analytical reagent grade. The silver colloidal SERS substrate was prepared by reducing  $\text{Ag}^+$  with hydroxylamine [11]. Briefly, 0.017 g silver nitrate were solved in 90 ml deionized water. In a separate recipient, 0.017 g of hydroxylamine hydrochloride were solved in 10 ml water, followed by the addition of 0.250 ml sodium hydroxide solution, 2 mol/l (v). The hydroxylamine/sodium hydroxide solution was then added rapidly to the silver nitrate solution under vigorous stirring. After few seconds a grey-brown colloidal solution resulted and it was further stirred for 10 minutes. The pH value of the silver colloid, measured immediately after preparation, was found to be 8.5.

The molecular geometry optimization, molecular electrostatic potential (MEP) and vibrational spectra calculations were performed with the Gaussian 03W software package [12] by using density functional theory (DFT) methods with B3LYP hybrid exchange-correlation functional [13, 14] and the standard 6-31G(d) basis set. No symmetry restriction was applied during geometry optimization. The vibrational frequencies were computed at the optimized geometry to ensure that no imaginary frequencies were obtained confirming that it corresponds to a local minimum on the potential-energy surface.

The assignment of the experimental frequencies are based on the observed band frequencies and intensity pattern of the Raman spectra and confirmed by establishing a one to one correlation between the observed and theoretical calculated frequencies. The calculated Raman activities ( $S_i$ ) were converted to relative Raman intensities ( $I_i$ ) using the following relationship [8-10]:

$$I_i = \frac{f(\nu_0 - \nu_i)^4 S_i}{\nu_i \left[ 1 - \exp\left(-\frac{hc\nu_i}{kT}\right) \right]} \quad (1)$$

where  $\nu_0$  is the exciting laser wavenumber,  $\nu_i$  is the wavenumber of the  $i$ -th vibrational mode,  $c$  is the speed of light,  $h$  and  $k$  are Planck's and Boltzmann's constants and  $T$  is the temperature.

For the plot of simulated Raman spectrum, pure Lorentzian band shapes were used with the full width at half height (FWHH) of  $15 \text{ cm}^{-1}$ . The last column in both Tables contains the motions that contribute the most to different normal modes according to B3LYP method coupled with the 6-31G(d) basis set. The computed wavenumbers have been scaled by 0.9614 as proposed by Scott and Radom [18]. To aid in mode assignment, we based on the direct comparison between the experimental and calculated spectra by considering both, the frequency sequence and intensity pattern, and by comparisons with vibrational spectra of similar compounds [19-22].

### 4.3

After geometry optimization, vibrational frequencies were calculated for amoxicillin; no imaginary frequencies were obtained for the optimized geometry given in Figure 1, and thus, it represents a true minimum on the potential energy surface.

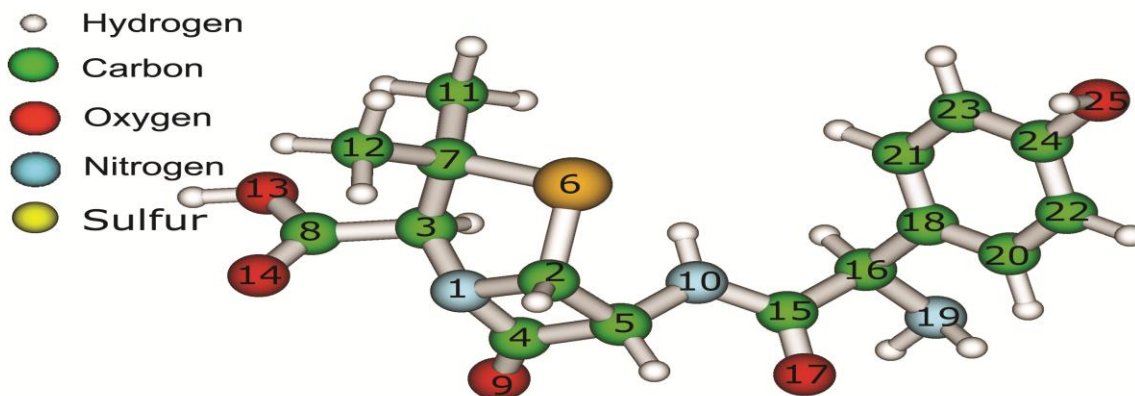


Figure 1. Optimized molecular structure and atom numbering scheme of amoxicillin.

#### Molecular electrostatic potential (MEP)

Molecular electrostatic potentials have been used for interpreting and predicting the reactive behavior of a wide variety of chemical systems in both electrophilic and nucleophilic reactions, the study of biological recognition processes and hydrogen bonding interactions [25, 26]. In this study, the amoxicillin atoms involved in the molecule adsorption to the silver surface are identified after analyzing the electrostatic potential map, as well. The MEP was calculated at the B3LYP/6-31G(d) optimized geometries, Figure 2 showing the calculated 3D electrostatic

tential contour map of amoxicillin in atomic units, the electron density isosurface being 0.02 a.u..

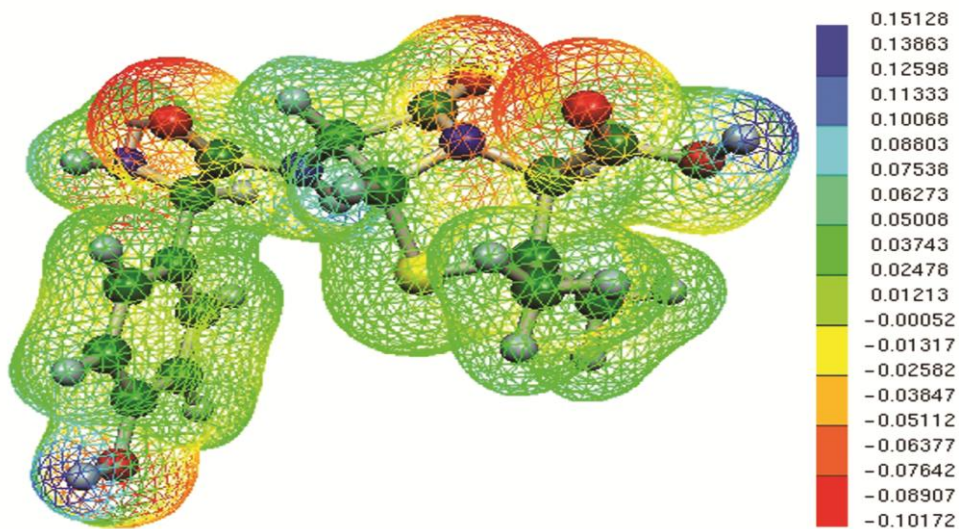


Figure 2. Calculated 3D molecular electrostatic potential contour map of amoxicillin, expressed in [au], as shown on the scale on the right side of the figure.

FTIR spectrum of amoxicillin: Fig.3 shows the experimental and calculated FTIR spectra of amoxicillin.

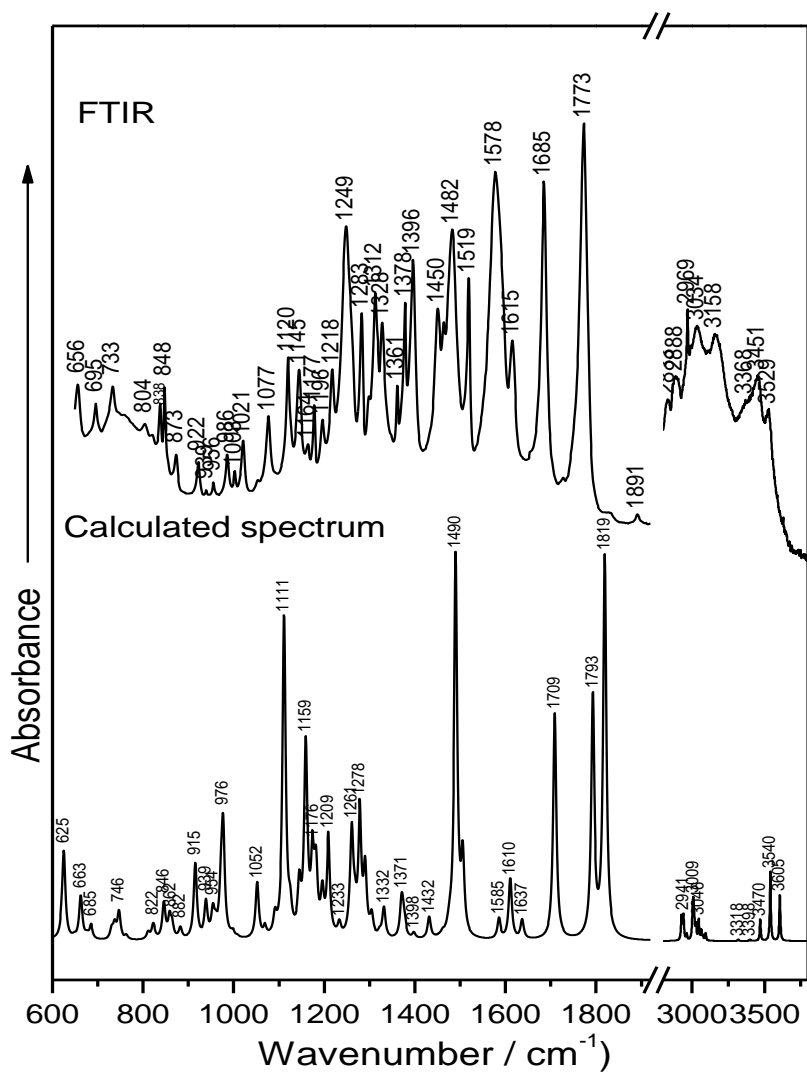


Figure 3. Experimental and calculated FTIR spectrum of amoxicillin.

For amoxicillin, the C=O stretching vibrations show intense IR absorptions, due to the considerable change in the molecular dipole moment produced by this vibration mode. Thus, the 1773 and 1685 cm<sup>-1</sup> bands, are due to the C8-O14 and C15-O17 stretching, as indicated by the theoretical DFT calculations. A detailed assignment of the experimental FTIR and calculated bands of amoxicillin is shown in Table 1.

Table 1.

Experimental FTIR and theoretical calculated IR bands of amoxicillin, as well as their assignment.

Experimental wavenumbers (cm <sup>-1</sup> ) 1)	Calculated wavenumbers (cm <sup>-1</sup> )	Band assignment
FTIR/ATR	B3LYP	
3529	3540	$\nu(\text{O13H})$
3451	3470	$\nu(\text{N10H})$
3368	3398	$\nu_{\text{as}}(\text{N19H}_2)$
3034	3046	$\nu_{\text{as}}(\text{C21H}, \text{C23H})$
2969	2963	$\nu(\text{C3H})$
1773	1793	$\nu(\text{C8O14}) + \delta(\text{O13H})$
1685	1709	$\nu(\text{C15O17}) + \delta(\text{N10H})$
1615	1610	$\nu(\text{CC ring2}) + \delta(\text{CH ring2})$
1578	1585	$\nu(\text{CC ring2}) + \delta(\text{CH ring2}) + \delta(\text{O25H})$
1482	1490	$\nu(\text{N10C15}) + \delta(\text{N10H}) + \delta(\text{C5H})$
1450	1432	$\nu(\text{CC ring2}) + \delta(\text{CH ring2}) + \delta(\text{O25H}) + \delta(\text{C16H})$
1396	1398	$\delta_{\text{s}}(\text{CH}_3)$
1378	1371	$\delta(\text{C3H}) + \delta(\text{C8O}_2\text{H}) + \nu(\text{C3C8})$
1328	1332	$\nu(\text{CC ring2}) + \delta(\text{CH ring2}) + \delta(\text{O25H})$
1283	1278	$\nu(\text{N1C3}) + \delta(\text{N10H}) + \delta(\text{N19H}_2) + \delta(\text{CH}) + \delta(\text{O13H})$
1249	1233	$\delta(\text{CH})$
1218	1209	$\nu(\text{C5C2}, \text{C5C4}, \text{C3N1}) + \delta(\text{N10H}) + \delta(\text{CH})$
1177	1176	$\delta(\text{N10H}, \text{N19H}_2) + \delta(\text{CH})$
1164	1159	$\delta(\text{CH ring2}) + \delta(\text{O25H}) + \delta(\text{CH}) + \delta(\text{N19H}_2)$
1120	1111	$\nu(\text{O13C8}) + \delta(\text{C8O14O13H}) + \delta(\text{O13H}) + \delta(\text{CH})$
1021	1052	$\nu(\text{CC}, \text{CN ring1}) + \nu(\text{N1C4}, \text{C2N1}) + \delta(\text{CH}) + \delta(\text{N19H}_2) + \delta(\text{C12H}_3)$
986	976	$\delta(\text{N19H}_2) + \text{op. bending CH ring2}$

956	954	$\delta(\text{CH})+\nu(\text{C16NH}_2)+\delta(\text{C15C16NH}_2)$
939	939	$\delta(\text{C8C3HN1})+\nu(\text{C8C3H,C2C5})+\delta(\text{CH})+$ $\delta(\text{O13H})+\delta(\text{N19H}_2)+\delta(\text{C12H}_3)$
922	915	$\nu(\text{C15C16H,C2C5})+\delta(\text{N19H}_2)+\delta(\text{C12H}_3)$
873	862	ring2 breathing $+\delta(\text{CH ring2})+\delta(\text{CH})+\delta(\text{N19H}_2)$
848	846	op. bending CH ring2
834	822	op. bending CH ring2
733	746	$\delta(\text{O13H})+\delta(\text{C8O}_2\text{H})+\rho(\text{CH}_3)+\nu(\text{C7C3})$
656	663	$\delta(\text{O13H})$

$\nu$ - stretch,  $\nu_s$ - symmetric stretch,  $\nu_{as}$ - asymmetric stretch,  $\delta$ - bending,  $\rho$ - rocking,  $\gamma$ -out-of-plane bending, def.-deformation, ip.-in plane, op.-out of plane, ring1: pyridine ring(N1-C2-S6-C7-C3); ring2: benzene ring(C18-C20-C21-C22-C23-C24)

As can be observed from Fig.3, other intense IR bands are those from  $1482\text{ cm}^{-1}$ , assigned mainly to N10C15 stretching and N10H bending, and  $1120\text{ cm}^{-1}$ , assigned mainly to O13C8 stretching and C8O14O13H bending vibration.

#### Raman and SERS spectra of amoxicillin

Figure 4 shows the FT-Raman, Raman DFT calculated and SERS spectra of amoxicillin.

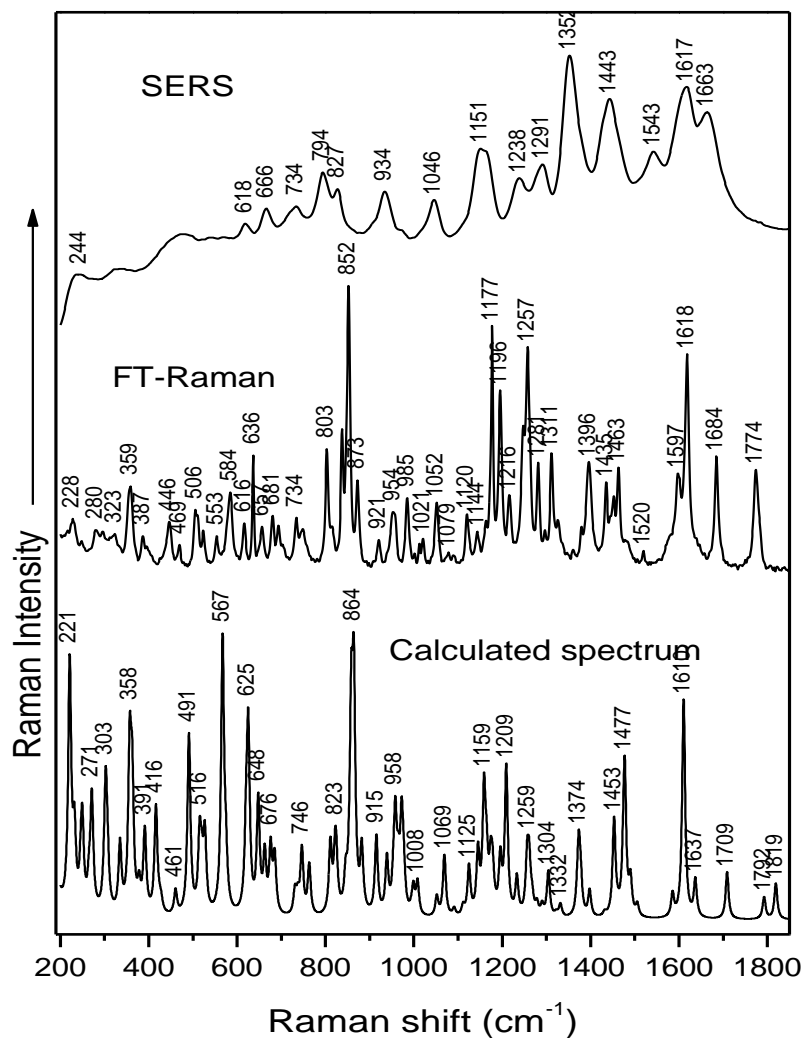


Figure 4. Experimental and simulated FT-Raman and SERS spectra of amoxicillin.

A good correlation between the theoretically calculated and FT-Raman bands can be observed. A detailed assignment of the experimental FT-Raman and SERS as well as of the DFT calculated Raman bands of amoxicillin are shown in Table 2. The FT-Raman and SERS bands were visually correlated with the calculated spectrum, by taking into account, both, wavenumber value and relative intensity, and thus the assignment of the FT-Raman and SERS spectrum was performed.

Table 2.

FT-Raman, SERS, and theoretical calculated (B3LYP/6-31G(d)) bands of amoxicillin, as well as their assignment.

Experimental wavenumbers (cm <sup>-1</sup> )		Calculated wavenumbers (cm <sup>-1</sup> )		Band assignment
SERS	FT-Raman	B3LYP		
244	228	221		$\rho(\text{NH}_2)+\rho(\text{CH}_3)$
	280	271		$\rho(\text{CNH}_2)+$ op. ring2 deformation
	323	303		$\rho(\text{CCH}_3)+\delta(\text{CCH}_3)$
	359	358		$\rho(\text{CCH}_3)+\delta(\text{CCH}_3)$
	387	391		op. ring2, ring1 deformation+op. ring2, ring1 bending
	446	416		ip. ring1 deformation+ $\delta(\text{COH})$
	469	461		ip. ring1 deformation+ $\delta(\text{NH})+\delta(\text{CCH}_3)$
	506	491		op. ring2 bending+ $\delta(\text{NH})$
	553	516		op. ring2, ring1 deformation+op. ring2, ring1 bending
	584	567		$\delta(\text{O13H})+\nu(\text{C7S6})+\delta(\text{C7CH}_3)+\delta(\text{CH}_3)$
618	616	625		$\delta(\text{O13H})+\delta(\text{CH})+\delta(\text{CH}_3)$
666	636	648		ip. ring2 deformation+ring2 breathing
734	734	746		$\delta(\text{O13H})+\delta(\text{C8O}_2\text{H})+\rho(\text{CH}_3)+\nu(\text{C7C3})$
794	803	811		ip. deformation
827	838	823		op. bending ring2+ $\delta(\text{CH ring2})$
	852	864		ring2 breathing+ $\delta(\text{CH ring2})+\delta(\text{CH})+\delta(\text{NH}_2)$
				$\rho(\text{NH}_2)+$ op. bending
934	921	915		ring1+ $\delta(\text{CH})+\nu(\text{C8C3})+\delta(\text{OH})$
	954	958		$\rho(\text{CH}_3)+$ op. bending CH ring2
	985	972		$\delta(\text{CH})+\nu(\text{C16NH}_2)+\delta(\text{C15C16NH}_2)$

	1021	1008	$\rho(\text{CH}_3)$
1046	1052	1069	$\nu(\text{C16NH}_2)+\delta(\text{NH}_2)+\delta(\text{CH})$
	1120	1125	$\delta(\text{C12C7C11})+\rho(\text{CH}_3)$
1151	1177	1159	$\delta(\text{CH})+\delta(\text{OH})+\delta(\text{CH ring2})+\nu(\text{CC ring2})$
	1196	1209	$\delta(\text{CH})+\delta(\text{NH})+\nu(\text{C5N10})$
1238	1257	1259	$\nu(\text{C24OH})+\delta(\text{CH ring2})$
			$\delta(\text{CH})+\delta(\text{NH})+\delta(\text{CH ring2})+\text{ip. ring2}$
	1311	1304	deformation
1352	1396	1374	$\delta(\text{CH})+\rho(\text{NH}_2)+\rho(\text{NH}_2\text{CH})$
1443	1435	1453	$\delta_{\text{as}}(\text{CH}_3)$
	1463	1477	$\delta_{\text{as}}(\text{CH}_3)$
1617	1618	1610	$\nu(\text{CC ring2})+\delta(\text{CH ring2})$
1663	1684	1709	$\nu(\text{C15O17})+\delta(\text{C16H})+\delta(\text{N10H})$
	1774	1792	$\nu(\text{C8O14})+\delta(\text{C3H})+\delta(\text{O13H})$

$\nu$ - stretch,  $\nu_s$ - symmetric stretch,  $\nu_{\text{as}}$ - asymmetric stretch,  $\delta$ - bending,  $\rho$ - rocking,  $\gamma$ -out-of-plane bending, def.-deformation, ip.-in plane, op.-out of plane, ring1: pyridine ring(N1-C2-S6-C7-C3); ring2: benzene ring(C18-C20-C21-C22-C23-C24)

Generally, the total symmetric vibration (breathing vibration) of aromatic rings shows high intensity Raman bands. In the FT-Raman spectrum of amoxicillin the total symmetric vibration of the benzene ring appears as a intense band at  $852\text{ cm}^{-1}$ , in the calculated Raman spectrum being present at  $862\text{ cm}^{-1}$ . Other intense FT-Raman bands in the amoxicillin spectrum are associated also with the benzene ring:  $1618\text{ cm}^{-1}$ , due to ring C=C stretching,  $1257\text{ cm}^{-1}$ , due to C-H bending and  $1177\text{ cm}^{-1}$ , due to C-C stretching and C-H bending.

## Adsorption geometry of amoxicillin to the silver surface

According to the surface-selection rules [23, 24], the normal modes, with a change in polarizability component perpendicular to the surface are enhanced. Theoretically, the interaction of amoxicillin with the silver surface can be established through the lone electron pairs of the O and N atoms, of the S atom, or through the  $\pi$  electrons of the rings.

The adsorption of amoxicillin to the silver surface is deduced based on the molecular electrostatic potential map and several marker bands. As can be seen in Figure 4 the highest electron density is located on oxygen atoms, thus the molecule is supposed to adsorb through the oxygen atoms. Benzene ring (ring 2) marker bands were identified at 852, 1177 and 1257  $\text{cm}^{-1}$ . These bands are less represented in the SERS spectrum, thus the benzene ring does not lie in the near vicinity of the silver surface. Intense bands in the SERS spectra are observed at 1352 and 1443  $\text{cm}^{-1}$  due to C-H bending and also at 1663 due to C=O stretching.

Thus, the adsorption of the molecule was deduced as presented in Figure 5.

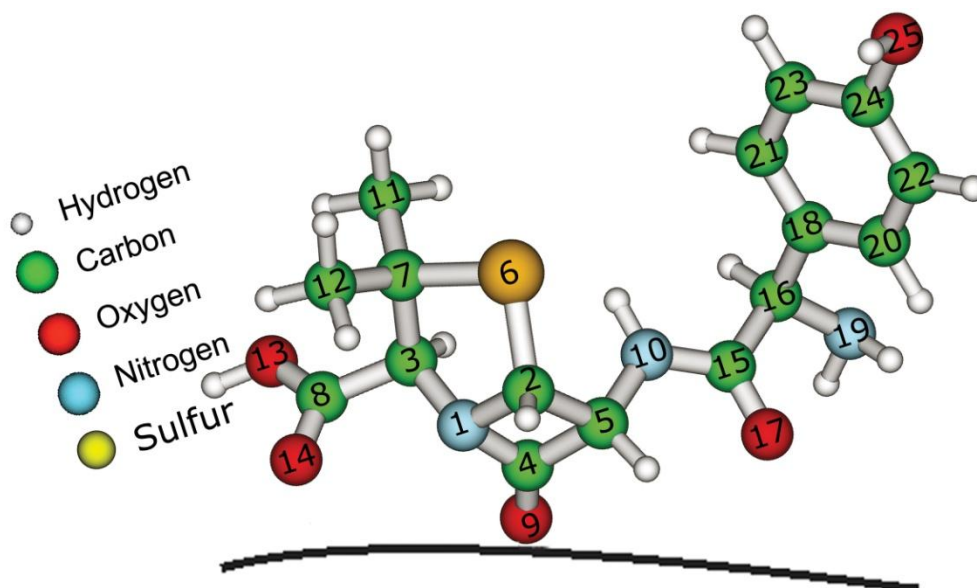


Figure 5. Schematically view of amoxicillin adsorption to the silver surface.

#### **4.4 Partial conclusions**

DFT calculations were employed for the geometry optimization, MEP and vibrational frequencies calculations of amoxicillin. The assignment of the FT-Raman and FTIR vibrational wavenumbers of amoxicillin was accomplished based on theoretical DFT calculations.

The adsorption geometry to the silver surface of amoxicillin was deduced from the SERS selection rules, several marker bands and the electrostatic potential map analysis.

## CONCLUSIONS

There have been synthesized three classes of metal complexes. The results of structural characterization of these complexes have been presented at various national conferences and have been materialized by publishing articles.

The purpose of synthesizing these compounds is their ability to further investigate the antibacterial, antifungal, anticancer and removal of residues from water.

The structural characterization of compounds with ligands of biomedical interest was achieved by techniques accessed, the elemental chemical analysis, atomic absorption mass, thermal measurements, Fourier transform infrared spectroscopy, ultraviolet and visible spectroscopy and electron spin resonance.

Given their bioapplicability were synthesized and characterized three metal complexes:  $[\text{Cu}(\text{C}_{15}\text{H}_{12}\text{N}_7\text{O}_4)_2] \cdot 8\text{H}_2\text{O}$ ,  $[\text{Co}(\text{C}_{15}\text{H}_{12}\text{N}_7\text{O}_4)_2] \cdot 8\text{H}_2\text{O}$  and  $[\text{Ni}(\text{C}_{15}\text{H}_{12}\text{N}_7\text{O}_4)_2] \cdot 8\text{H}_2\text{O}$  azoderivatives having as a ligand type  $\text{C}_{15}\text{H}_{12}\text{N}_7\text{O}_4$ .

Elemental chemical analysis and thermal analysis confirms the stoichiometry of the complexes and molar ratio M: L:  $\text{H}_2\text{O}$  = 1:2:8.

Infrared spectroscopy, ultraviolet and visible indicates that the organic ligand acts as bidentate compound, involving the coordination with metal ion atom of nitrogen from azo group and an oxygen atom linked pyrazole ring.

Electron spin resonance spectra confirms pseudotetraedral symmetry around the metal ions for the first class of complexes.

There have been synthesized and characterized the physico-chemical and spectroscopic 8 new Metal complex type  $[\text{M}(\text{HL})_n] \cdot x\text{H}_2\text{O}$  where  $\text{HL} = [\text{C}_2\text{HN}_2\text{S}_3\text{CH}_2\text{COO}]^-$  - and  $\text{M} = \text{Mn}^{2+}$ ,  $\text{Co}^{2+}$ ,  $\text{Ni}^{2+}$ ,  $\text{Cu}^{2+}$ ,  $\text{Zn}^{2+}$ ,  $\text{CR}^{3+}$ ,  $\text{Fe}^{3+}$  and  $\text{Ag}^+$ .

Microanalysis confirms the stoichiometric ratio and analytical purity of all the eight newly synthesized complexes.

FT-IR spectroscopy confirms the bidentate ligand and allows to define their coordination to metal centers. This ligand acts as monoanionici carboxylates, containing a group in its protonated tioamidic dent.

Electronic spectra and electron spin resonance of the complexes, measured at room temperature, confirming the metal-ligand covalent bonds formed, or pseudooctaedral octahedral

symmetry around the metal ions. Giromagnetic tensors values correspond to chromophore type  $MO_6$  with contributions from oxygen atoms derived from carboxyl groups and the water molecules.

Spectroscopic methods cannot provide enough information about how metals bind to proteins, understanding the nature of amino acids link metal can get very useful information about proteins by metal coordination.

In this context we have synthesized and characterized from the physico-chemical, thermal and spectroscopic Nov. metal complexes in aqueous solutions such as:  $Cu(L)_2 \cdot H_2O$ ,  $Co(L)_2 \cdot 2H_2O$  and  $Zn(L)_2 \cdot H_2O$ , where L = phenylalanine.

Elemental chemical analysis, atomic absorption mass and thermal analysis confirms the stoichiometry of the complexes and molar ratio M: L:  $H_2O$  = 1:2:1 for copper and zinc complexes and M: L:  $H_2O$  = 1:2:2 for those cobalt.

Comparison of FT-IR spectra of compounds synthesized amino acids and allowed to define their coordination to metal centers via amino nitrogen atom and oxygen atom of carboxyl group. Also, analysis of vibration bands at about  $3600\text{ cm}^{-1}$  allowed the determination of the number of water molecules which coordinates the metal center. Were identified and assigned to the main vibration bands of significant molecular groups. IR spectra indicate bidentate nature of the ligands and allowing a local geometry pseudotetraedral for ions Cu (II) and Zn (II) and one for octahedral complexes of Co (II). Octahedral local symmetry for ions Co (II) coordination is done by the axial position of two water molecules.

Electronic spectra and electron spin resonance of complexes, powder measured at room temperature, confirming the metal-ligand covalent bonds formed, pseudotetraedral symmetry around copper and zinc ions and the surrounding octahedral for cobalt.

The results obtained so far justify further research, both in terms of solving structures in solid and in solution and in the biological activity of these compounds.

## **AK NOLEDGEMENTS**

There are a lot of people to whom I want to thank - people who actually helped me and encouraged me to carry out this work. To all of them I am grateful.

First I want to thank Mr. Prof. Dr. David Leontin who always supported me and believed in me and in this paper. Without him by my side it would have been much harder.

I am grateful to the Biomedical Physics Department staff and especially to Mr. Dean Prof. Dr. ONUC Cozar because he gave me confidence and full support which I needed to complete this thesis.

I had a very good collaboration with members of this department who have supported me and helped me with advice and continuous support in writing articles.

Many thanks to Prof.Dr. Vasile Chis, Mrs.Dr. Simona Pinzaru, Mr.Lecturer. Dr.Nicholas Leopold, Mr. phys. Dr.Laci Szabo for constant and prompt help whenever I needed.

All my appreciation and good thoughts are heading towards my parents, Mihai and Dorina Bebu, for support and understanding shown with generosity in these years.

Finally I want to thank the doctoral program: "Through Science to Society", POSDRU contract 6/1.5/S/3 for financial support in completing this thesis.

This paper is for all those who over time I have asked questions, they asked me for help, have praised or criticized me, encouraging me to prepare myself that way permanently.